

S-Glutathionylation of Cryptic Cysteines Enhances Titin Elasticity by Blocking Protein Folding

Jorge Alegre-Cebollada,^{1,6,*} Pallav Kosuri,^{1,2,6} David Giganti,¹ Edward Eckels,^{1,3} Jaime Andrés Rivas-Pardo,¹ Nazha Hamdani,⁴ Chad M. Warren,⁵ R. John Solaro,⁵ Wolfgang A. Linke,⁴ and Julio M. Fernández^{1,*}

¹Department of Biological Sciences, Columbia University, New York, NY 10027, USA

²Graduate Program in Biochemistry and Molecular Biophysics, Columbia University, New York, NY 10032, USA

³Columbia College of Physicians and Surgeons, Columbia University, New York, NY 10032, USA

⁴Department of Cardiovascular Physiology, Ruhr University Bochum, 44780 Bochum, Germany

⁵Department of Physiology and Biophysics, College of Medicine, University of Illinois at Chicago, Chicago, IL 60612, USA

⁶Co-first authors

*Correspondence: ja2544@columbia.edu (J.A.-C.), jfernandez@columbia.edu (J.M.F.)

<http://dx.doi.org/10.1016/j.cell.2014.01.056>

SUMMARY

The giant elastic protein titin is a determinant factor in how much blood fills the left ventricle during diastole and thus in the etiology of heart disease. Titin has been identified as a target of S-glutathionylation, an end product of the nitric-oxide-signaling cascade that increases cardiac muscle elasticity. However, it is unknown how S-glutathionylation may regulate the elasticity of titin and cardiac tissue. Here, we show that mechanical unfolding of titin immunoglobulin (Ig) domains exposes buried cysteine residues, which then can be S-glutathionylated. S-glutathionylation of cryptic cysteines greatly decreases the mechanical stability of the parent Ig domain as well as its ability to fold. Both effects favor a more extensible state of titin. Furthermore, we demonstrate that S-glutathionylation of cryptic cysteines in titin mediates mechanochemical modulation of the elasticity of human cardiomyocytes. We propose that post-translational modification of cryptic residues is a general mechanism to regulate tissue elasticity.

INTRODUCTION

The sarcomeric protein titin determines the passive elasticity of heart muscle and is crucial for proper cardiac function, for example, during diastolic relaxation of the left ventricle (Linke and Krüger, 2010). The key role of titin in the homeostasis of striated muscle is illustrated by the recent discovery that truncations in the titin gene are a primary cause of dilated cardiomyopathies and centronuclear myopathy (Ceyhan-Birsoy et al., 2013; Herman et al., 2012; McNally, 2012; Norton et al., 2013). In addition, a growing number of missense mutations in the elastic I-band of titin are known to cause several forms of cardiomyopathy by mechanisms that remain poorly understood (Anderson et al.,

2013; Gerull et al., 2002; Itoh-Satoh et al., 2002; Matsumoto et al., 2005; Taylor et al., 2011). The elasticity of muscle is adapted to its physiological needs via changes in titin. For instance, the 363 exons contained in the titin gene can be alternatively spliced to obtain different isoforms with tailored elastic properties (Freiburg et al., 2000). However, it remains largely unexplored how the elasticity of titin is regulated in short timescales that are not compatible with protein turnover.

The elastic I-band of titin is composed of up to 100 folded immunoglobulin (Ig) domains linked in series. Occasionally, unstructured polypeptide regions can be found interspersed between the Ig domains (Figure 1A). Titin employs two complementary mechanisms to adapt its length to the changing mechanical perturbations during heartbeats: entropic extension/recoil of the unstructured regions and unfolding/refolding of Ig domains (Li et al., 2002). Although the extent of Ig unfolding/refolding during muscle action was a matter of debate for several years, today the consensus in the field is that unfolding/refolding of at least some titin domains occur in vivo and contribute to the overall elasticity of titin (Anderson et al., 2013; Li et al., 2002; Minajeva et al., 2001; Nedrud et al., 2011; Trombitás et al., 1998). Unfolding of Ig domains decreases titin stiffness because the residues belonging to the unfolded domains add to the pool of unstructured regions, which are easy to extend under force. In contrast, refolding of Ig domains increases titin stiffness. Phosphorylation and disulfide formation at specific residues belonging to the unstructured regions can provide some degree of regulation of titin elasticity (Linke and Krüger, 2010). To attain larger changes in elasticity, a regulatory mechanism would have to target the mechanical properties of the much more abundant Ig domains. Any variation in their mechanical stability or their refolding kinetics would lead to changes in the overall elasticity of titin, as both effects determine the residence time of Ig domains in the unfolded state.

Titin has been identified as a likely target of increased S-glutathionylation following myocardial infarction (Avner et al., 2012), a pathology that is accompanied by augmented elasticity of the left ventricle (Pfeffer and Braunwald, 1990). S-glutathionylation is the end product of many redox signaling pathways, including

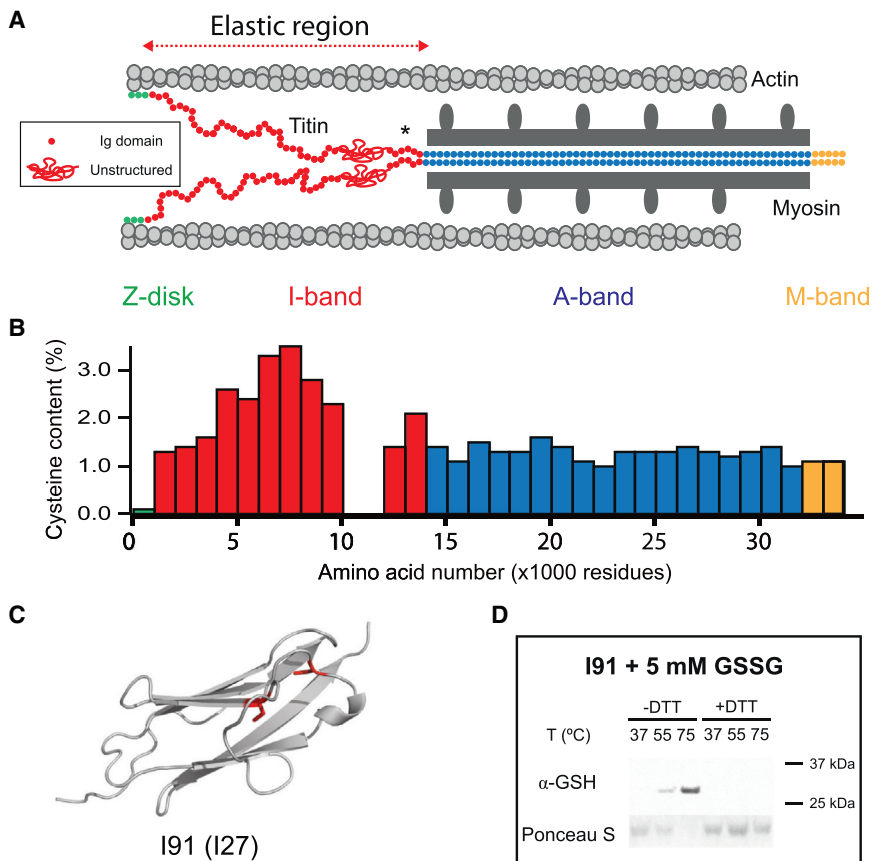


Figure 1. Ig Domains in the I-Band of Titin Are Rich in Cryptic Cysteines

(A) Schematic representation of a half-sarcomere. Titin (in color) extends from the Z-disk to the M-band of the sarcomere. The approximate location of the I91 domain is indicated with an asterisk.

(B) Average cysteine content in the titin sequence. (C) Structure of the titin I91 domain (also known as I27; PDB code 1TIT), highlighting in red its two cysteine residues.

(D) The cysteines in I91 are cryptic and can only be S-glutathionylated after unfolding. A SUMO-I91 construct was incubated with GSSG for 1 hr at different temperatures. S-glutathionylation was determined by western blotting and labeling with anti-glutathione antibodies (α -GSH). Ponceau S shows the total protein content. See also Figure S1.

However, the use of standard range SDS-PAGE gels precluded definitive identification of titin due to its large size. To improve resolution in the high-molecular-weight region, we repeated these experiments using better-suited SDS-vertical agarose gels (Warren et al., 2003). After western blotting, we identified bands with the expected electrophoretic mobility of titin that react both with anti-titin and with anti-glutathione antibodies. Incubation with the reducing agent beta-mercaptoethanol to revert

S-glutathionylation selectively prevented binding of the anti-glutathione antibody (Figure S1A available online). These results confirm that titin is S-glutathionylated in vivo.

nitric oxide signaling (Dalle-Donne et al., 2009; West et al., 2006), which are well-recognized regulators of cardiac muscle and its elasticity (Hare, 2004; Rastaldo et al., 2007). Previous studies have shown that active contraction of muscle is regulated by S-glutathionylation of ryanodine receptor 2 (Sánchez et al., 2005) and sarcomeric proteins such as actin (Chen and Ogut, 2006), troponin I (Mollica et al., 2012), and myosin-binding protein C (Lovell et al., 2012). However, the potential effects of S-glutathionylation on the passive mechanical properties of cardiac muscle remain unexplored.

Here, we examine the link between S-glutathionylation of titin and changes in the elasticity of cardiac muscle. We show that S-glutathionylation of cryptic cysteines, which are exposed upon unfolding of titin's Ig domains, causes increased elasticity of titin through mechanical weakening and inhibition of folding. These changes in titin's mechanical properties lead to a marked decrease in the stiffness of cardiomyocytes.

RESULTS

Titin Is a Target of S-Glutathionylation

Covalent modification of cysteine residues including S-glutathionylation is a typical outcome of redox signaling (Hare, 2004; Martínez-Ruiz and Lamas, 2007). S-glutathionylation has been shown to target a very high-molecular-weight protein in murine cardiac tissue, putatively identified as titin (Avner et al., 2012).

Cryptic Cysteines in Titin

The amino acid sequence of the Ig domains in the elastic I-band of titin is highly abundant in cysteine residues, all of which are potential targets for S-glutathionylation (Figure 1B; Kellermayer and Grama, 2002). All I-band Ig domains of titin whose structure has been determined, I1 (Protein Data Bank [PDB] code 1G1C), I65-I70 fragment (PDB code 3B43), and I91 (also known as I27; PDB code 1TIT; Figures 1A and 1C), contain at least two cysteine residues that appear to be buried. Some of these cysteines are clustered and have the potential to engage in disulfide bonds (Mayans et al., 2001), whereas others are far from each other, as in the case of Cys47 and Cys63 in I91 (Figure 1C). To obtain information about the location of cysteine residues in the remaining domains, we carried out homology modeling of all Ig domains in the I-band of the canonical human titin gene (Uniprot code: Q8WZ42). Our analysis predicts that 89 out of 93 Ig domains in the I-band of titin contain cryptic cysteines. These cysteines would only become modified by redox-active molecules if the protein domains first unfold (Figure S1B).

We tested experimentally whether the cysteines in I91 are accessible to redox modification by incubation with oxidized glutathione (GSSG). A cysteine residue reacts with GSSG via

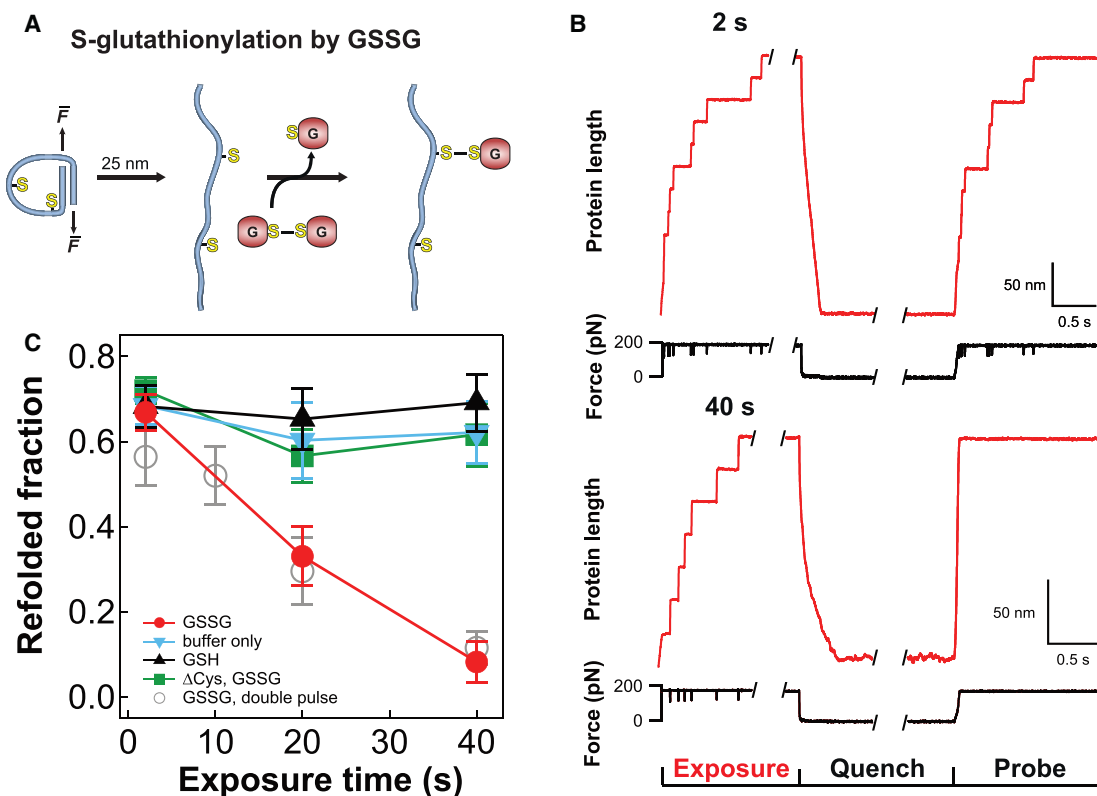


Figure 2. S-Glutathionylation of Cryptic Cysteines Inhibits Refolding of I91

(A) I91 contains two cryptic cysteines that become exposed by mechanical unfolding. At a force of 130–175 pN, the unfolding of an I91 domain can be identified as a 25 nm step increase in end-to-end length. Exposure of the unfolded protein to GSSG leads to S-glutathionylation.

(B) A single polyprotein is unfolded at 175 pN in 100 mM GSSG and then held extended for a variable length of time (exposure time; 2 s top trace; 40 s bottom trace). The force is then quenched to zero for 5 s to allow the protein to refold. We measure the extent of refolding by applying a probe pulse.

(C) Refolded fraction as a function of exposure time for I91₈ polyproteins exposed to buffer only (downward triangles; $n > 35$), 100 mM GSSG (solid circles; $n > 80$), 200 mM GSH (upward triangles; $n > 80$) and refolded fraction in the presence of 100 mM GSSG for a mutant I91₈ polyprotein where all cysteine residues were replaced by alanines (Δ Cys, squares; $n > 120$). The refolded fraction was calculated as the ratio between the number of unfolding steps detected during the probe pulse and the number of unfolding steps detected during the exposure pulse. Open symbols represent total refolding of I91 (weak + strong domains) in the presence of 100 mM GSSG, as determined using the double-probe pulse protocol in Figure 3. Error bars represent SEM.

simple thiol/disulfide exchange (Gilbert, 1990). We incubated I91 in 5 mM GSSG at different temperatures and then detected S-glutathionylation through western blotting and staining using anti-glutathione antibodies. We found that I91 does not react with GSSG at 37°C, implying that the cysteines in native I91 are inaccessible to GSSG under physiological conditions (Figure 1D). However, I91 became S-glutathionylated at temperatures higher than 55°C, which have been shown to unfold I91 (Somkuti et al., 2013; Figure 1D). S-glutathionylation could be reversed by incubation with 50 mM dithiothreitol (DTT), a strong reducing agent that cleaves the mixed disulfide between cysteine and glutathione (Figure 1D). These results confirm that the cysteines in I91 are buried and can only be S-glutathionylated when exposed to the solvent through protein unfolding. According to our homology models, similar results are expected for the majority of Ig domains in titin.

Cysteines found in buried positions are typically regarded as inert and not seen as potential targets of redox signaling. However, proteins that experience mechanical forces can be

unfolded in cells (del Rio et al., 2009; Johnson et al., 2007; Li et al., 2002; Smith et al., 2007). Hence, the mechanical unfolding of a protein can expose cryptic cysteines that are normally inert, making them reactive (Johnson et al., 2007; Klotzsch et al., 2009). We hypothesized that mechanical unfolding can enable covalent modification of titin's cryptic cysteines, which would disrupt the folding/unfolding dynamics and cause sustained changes in titin elasticity. We set out to test this hypothesis using force-clamp spectroscopy by atomic force microscopy (AFM), a single-molecule technique that mimics the mechanical perturbations experienced by titin domains in the heart (Fernandez and Li, 2004; Li et al., 2002).

S-Glutathionylation of Cryptic Cysteines Inhibits Folding of I91

We first investigated the effects of S-glutathionylation on the refolding of I91. We mechanically unfolded and extended I91 polyproteins at a constant force of 175 pN (exposure pulse) in the presence of 100 mM oxidized glutathione (GSSG; Figure 2).

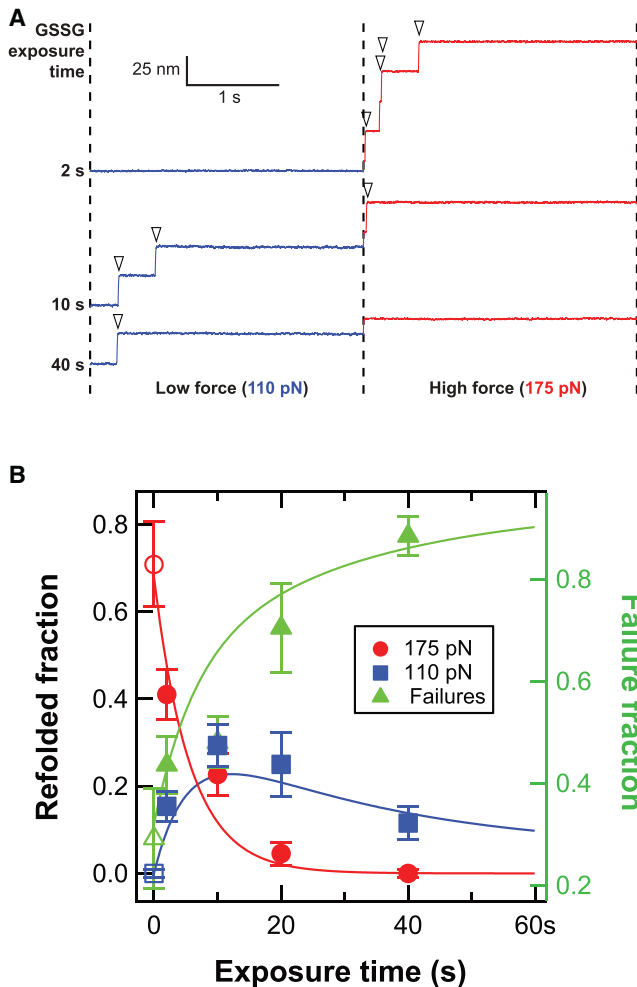


Figure 3. Graded Mechanical Modulation of I91 by S-Glutathionylation

(A) Experimental recordings showing unfolding steps during the probe pulse (open arrowheads). Each recording was obtained in 100 mM GSSG after a different exposure time followed by 5 s refolding. Refolded domains with different mechanical stability were detected using a two-level probe pulse (110 pN in blue followed by 175 pN in red).

(B) Refolded fraction (circles and squares; left axis) and failures (triangles; right axis) as a function of exposure time ($n > 40$). Squares indicate weak domains detected during the low-force regime; circles indicate native domains detected in the high-force regime. Data points at zero exposure time were obtained in buffer without GSSG (open symbols; $n = 24$). Solid lines were obtained from the kinetic model shown in Figure 5A. Error bars represent SEM. See also Figure S2.

Under force, 25 nm step increases in length mark the mechanical unfolding and extension of one I91 domain in the polyprotein (Figure 2A). Unfolding of multiple domains produces staircase-like changes in length, which we used to fingerprint single-molecule events (Figure 2B). Mechanical unfolding exposes both buried cysteines, which become reactive toward GSSG in the solution, resulting in S-glutathionylation (Figure 2A). We kept the cysteines exposed for variable amounts of time by changing the duration of this exposure pulse (Figures 2B and 2C). We then

ended the exposure by quenching the force to 0 pN for 5 s, allowing for the collapse and folding of the I91 polyprotein (quench pulse; Figure 2B). We quantified folding with a probe pulse (175 pN; Figures 2B and 2C). The presence of a second staircase of 25 nm steps marks the successful refolding of the protein. When the exposure time was brief (2 s; Figure 2B, top trace), folding proceeded successfully. However, when the exposure time was increased (40 s; Figure 2B, bottom trace), allowing for extensive S-glutathionylation of the unfolded protein, unfolding steps were no longer observed during the probe pulse, indicating impaired folding. The near-complete inhibition of refolding observed after 40 s exposures to GSSG was not seen in the presence of reduced glutathione or with buffer alone (Figure 2C). To verify that the refolding inhibition was caused by cysteine modification, we repeated the experiment with a cysteine-free I91 mutant. Refolding of this mutant was not affected by exposure to GSSG (Δ Cys; Figure 2C). Taken together, these results show that S-glutathionylation of the cryptic cysteines in I91 inhibits protein folding.

S-Glutathionylated I91 Domains Can Fold into a Weakened State

We noticed that, in the presence of GSSG, unfolding events often appeared faster in the probe pulse than in the exposure pulse. This observation led us to believe that some of the glutathionylated domains had refolded into mechanically weakened structures. In order to detect discrete populations of folded domains with different mechanical stabilities, we modified the probe pulse to consist of a force ramp from 0 pN to 200 pN. In the absence of GSSG, most of the refolded I91 domains unfolded at 150–200 pN. Strikingly, when the buffer contained GSSG, we detected a second population of refolded I91 domains that unfolded at much lower forces of around 100 pN (Figure S2).

To quantify the incidence of weak and native I91 domains independently, we modified the probe pulse to include two regimes of constant force (110 pN and 175 pN; Figure 3A). We designed this protocol so that only weak domains would unfold during the initial low force pulse, whereas natively folded domains would unfold only after application of the high force. Indeed, for short exposure pulses (2 s; Figure 3) or in the absence of GSSG, the majority of the 25 nm steps are observed during the high-force regime of the probe pulse, indicating mostly native folding (circles; Figure 3B). Meanwhile, for exposure pulses longer than 10 s, the majority of the 25 nm steps occur during the low-force pulse (Figure 3A). Longer exposure pulses led to overall fewer 25 nm steps in the probe pulses (Figure 3B). The total refolding fractions detected using the single- and double-probe pulse protocols are coincident, indicating that we detected all refolded domains in both experiments (Figure 2C).

Given that 25 nm steps are fingerprints of folded domains, their absence from the probe pulse can be used to detect domains that failed to fold. We counted the failures (triangles; Figure 3B) as the number of unfolding steps in the exposure pulse minus the number of unfolding steps in the probe pulse. The failures became more frequent with increasing exposure time. Meanwhile, the population of weakened domains peaked at an exposure time of 10 s (Figure 3B). This transient increase in weakened domains followed by complete inhibition of folding

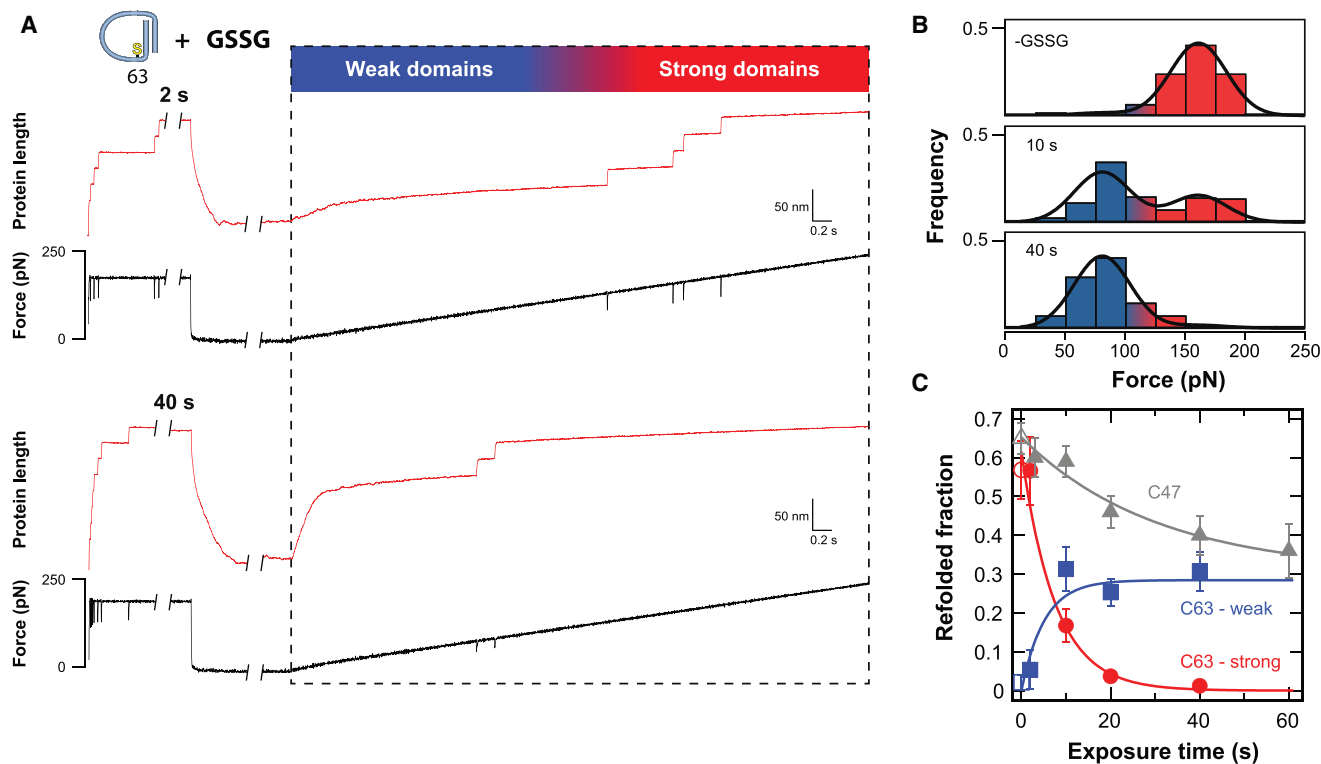


Figure 4. S-Glutathionylation of Different Cysteines Produces Distinct Mechanical Phenotypes

(A) The single-cysteine mutant I91-Cys63 was mechanically unfolded and exposed to 100 mM GSSG for a variable amount of time. After a 5 s quench to allow for folding, refolding was probed using a linear force ramp up to 240 pN.

(B) Mechanical stability of refolded I91-Cys63 after varying exposure times to 100 mM GSSG ($n > 25$). Solid lines indicate fits of Gaussians with fixed widths and centroids.

(C) Refolded fraction of I91-Cys47 (triangles; $n > 120$) and I91-Cys63 (weak domains, squares; strong domains, circles; $n > 150$) at different exposure times for a fixed quench time of 5 s in 100 mM GSSG. Data points at zero exposure time were obtained in the absence of GSSG (open symbols; $n > 150$). Reaction rates of S-glutathionylation were measured from exponential fits (solid lines). Error bars represent SEM.

See also [Figure S3](#).

indicates the presence of at least three states, which is consistent with the two potential S-glutathionylation sites in each I91 domain. The results can be explained by a scenario in which S-glutathionylation of one cysteine in I91 weakens the domain while S-glutathionylation of the second cysteine abolishes mechanical stability altogether.

The Mechanical Effects of S-Glutathionylation Are Site Specific

We set out to characterize the effects of S-glutathionylation at each of the two cysteines in I91. We conducted refolding experiments using single-cysteine mutants of I91 in which one of the cysteines had been mutated to alanine. We refer to these mutants as I91-Cys47 (C63A) and I91-Cys63 (C47A), respectively, highlighting the remaining cysteine in each case. The probe pulse consisted of a ramp from 0 to 240 pN in 6 s, which allowed us to assess the mechanical stability of the refolded domains ([Figures 4](#) and [S3](#)). Exposure of I91-Cys63 to GSSG for short periods of time led to refolded domains with native mechanical stability, whereas longer exposure times led to weak refolded domains that unfolded at a lower force ([Figures 4A](#), [4B](#), and

[S3B](#)). Weak domains were not observed for I91-Cys47, even after exposure times in excess of 40 s ([Figure S3A](#)). We conclude that the weak domains seen upon S-glutathionylation of I91 wild-type (WT) are due to modification of Cys63 specifically. If we assume similar exponential force dependence, these weak domains would unfold at a rate two orders of magnitude faster compared to native domains at any given force ([Figure S3C](#)).

The abundance of weak domains in I91-Cys63 reached a constant value after ~ 10 s and did not disappear at longer exposure times ([Figure 4C](#)). The persistence of these weak domains contrasts with I91 WT, where the appearance of weak domains was transient ([Figure 3B](#)). We conclude that disappearance of weak I91 WT domains at longer exposure times was likely caused by a second S-glutathionylation, at Cys47.

S-glutathionylation at either Cys47 or Cys63 leads to a decrease in total refolding ([Figure 4C](#)). To investigate if this decrease could be explained by a decrease in folding kinetics, we measured the folding rate of S-glutathionylated I91-Cys63 ([Figure S3D](#)). First, we unfolded the protein for 20 s in the presence of GSSG to allow for ample S-glutathionylation. We then quenched the force for a variable amount of time and probed

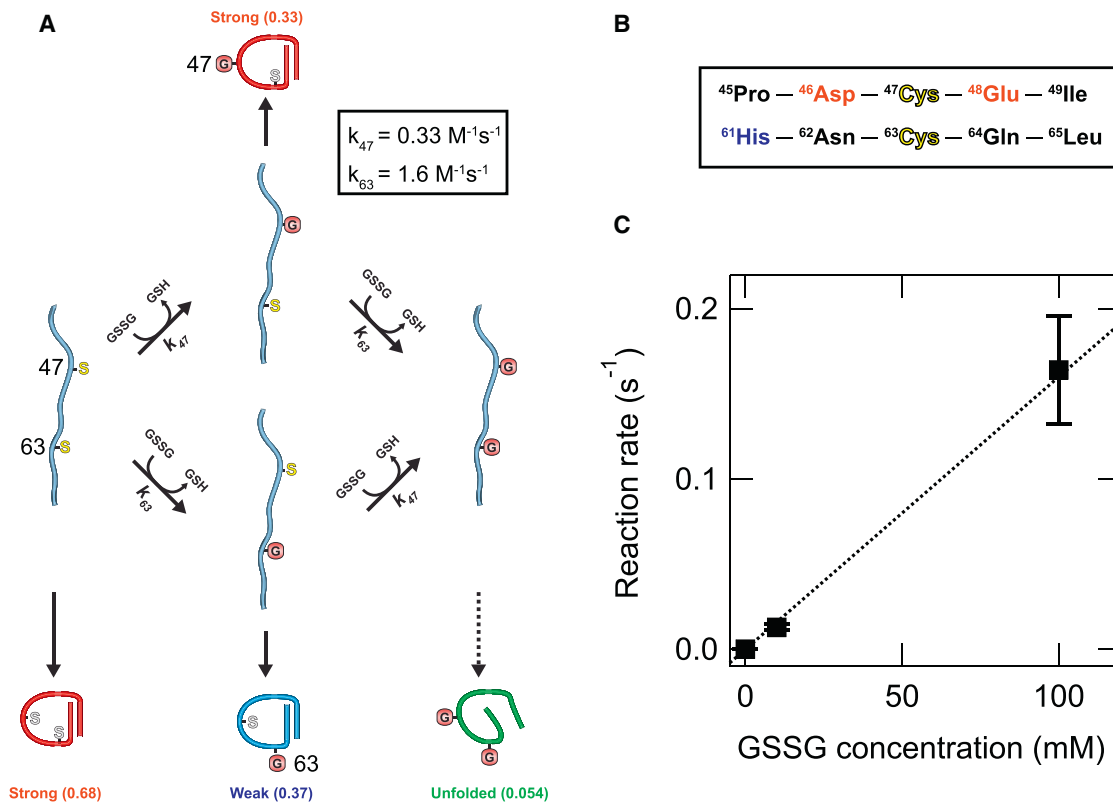


Figure 5. Kinetic Model

(A) Scheme that includes all possible reaction pathways for S-glutathionylation and mechanical outcomes. Numbers in parentheses are the asymptotic folding fractions.

(B) Sequence flanking the two cysteines in I91. Negatively charged residues are labeled red; positively charged residues are labeled blue.

(C) The rate of S-glutathionylation of Cys63 depends linearly on the concentration of GSSG. Error bars represent SEM.

See also [Figure S4](#).

refolding after a variety of quenching times. The folding rate of S-glutathionylated I91-Cys63 appears indistinguishable from the folding rate of the unmodified protein ([Figure S3D](#)). Hence, the decrease in refolding was not caused by altered folding kinetics. Instead, it appeared that a fraction of the glutathionylated domains simply fail to fold at all. One possibility is that, during refolding, S-glutathionylated domains have a stronger tendency to become trapped in off-pathway misfolded states that do not mature into folded, mechanically stable structures.

Because folding rates appeared unchanged by S-glutathionylation, we took advantage of the decrease in overall folding to measure the site-specific rates of S-glutathionylation. We found that the first-order rate of glutathionylation at Cys63 was nearly five times higher than the glutathionylation at Cys47 ([Figures 4C and 5A](#)). The lower reactivity of Cys47 is likely caused by the presence of negatively charged neighboring residues ([Figure 5B](#); [Wu et al., 2011](#)). Refolding measurements of I91-Cys63 in the presence of 10 mM GSSG confirmed that the glutathionylation rate changes linearly with the concentration of GSSG, as expected for a first-order chemical reaction ([Figures 5C and S4](#)).

Based on our results with the single-cysteine mutants, we constructed a kinetic model that predicts the mechanical outcomes of S-glutathionylation in I91 WT ([Figure 5A](#)). The model

contains two classes of parameters: amplitude of folding of each of the four states of glutathionylation and site-specific glutathionylation rates k_{47} and k_{63} . The only free parameter in the model is the extent of refolding of the doubly glutathionylated I91 WT. The value of this parameter was determined through numerical optimization. We found that a value of 0.054 best fits the I91 WT data ([Figure 3B](#)), confirming that folding is severely compromised in the doubly glutathionylated I91.

The Mechanical Effects of S-Glutathionylation Are Reversed by the Enzyme Glutaredoxin

Reversible S-glutathionylation is emerging as an important downstream regulatory posttranslational modification in various redox signaling pathways ([Dalle-Donne et al., 2009](#)). Although several chemical and enzymatic pathways can lead to S-glutathionylation ([Gallogly and Mieyal, 2007](#)), deglutathionylation is mainly the result of the activity of specific enzymes, primarily glutaredoxin (GRX) ([Lillig et al., 2008](#)). Hence, we reasoned that GRX could rescue refolding following S-glutathionylation of I91. To test this hypothesis, we used an alternative pathway of S-glutathionylation that is compatible with the activity of GRX. A protein-glutathione complex can be obtained through the attack of a free cysteine on GSSG but also through the cleavage of a protein

disulfide bond by a reduced glutathione molecule (GSH). We took advantage of this latter route because it allows S-glutathionylation in a reducing buffer, necessary to preserve GRX activity. Because the cysteines in I91 WT are far apart and do not establish a disulfide bond, we used the mutant I91₃₂₋₇₅. This I91 mutant readily forms a buried disulfide bond between engineered cysteines at positions 32 and 75. The disulfide in I91₃₂₋₇₅ becomes exposed and reactive only upon mechanical unfolding (Wiita et al., 2006; Kosuri et al., 2012; Figure 6).

When an I91₃₂₋₇₅ protein domain is placed under a constant stretching force of 150 pN, unfolding yields an 11 nm stepwise increase in length, resulting in the exposure of the buried disulfide (Wiita et al., 2006). Cleavage of the exposed disulfide by GSH further increases the length of the protein by 14 nm, providing an unambiguous fingerprint for S-glutathionylation (Figures 6A and 6C). Figure 6A shows a recording where an I91₃₂₋₇₅ polyprotein is first unfolded and S-glutathionylated and then allowed to collapse and refold. Twenty-five nanometer steps in the probe pulse indicate a refolded protein without disulfide. S-glutathionylated domains did not refold well, as 25 nm steps were only rarely seen in the probe pulse (Figures 6A and 6E). Those few domains that refolded showed native mechanical stability (Figures S5A–S5C). We repeated the glutathionylation-refolding experiment but now in the presence of GRX in conditions where the enzyme does not effectively cleave disulfide 32–75 (Figures 6B, 6D, and S5D). S-glutathionylated proteins exposed to 45 μ M GRX showed robust refolding similar to controls using reduced I91₃₂₋₇₅ in the presence of GSH, a condition where S-glutathionylation is not possible (Figure 6E). The rescue of protein folding by GRX shows that the mechanical effects of I91 S-glutathionylation are reversible.

S-Glutathionylation of Cryptic Cysteines Decreases the Stiffness of Human Cardiomyocytes

Our homology models suggest that almost all Ig domains in the I-band of titin contain cryptic cysteines (Figure S1B). We have shown that S-glutathionylation of cryptic cysteines softens domain I91 by inhibiting refolding and inducing a mechanically weak state (Figures 2, 3, 4, and S2). Hence, if I91 is a good representative of the many cryptic-cysteine-containing domains in titin, then S-glutathionylation would lead to large-scale changes in the elasticity of titin by inducing extensive softening of its Ig domains. Because titin is the major contributor to the passive elasticity of cardiomyocytes (Linke et al., 1994), we reasoned that the elasticity of cardiomyocytes could be regulated through posttranslational modification of titin's cryptic cysteines. To test our hypothesis, we measured the passive elasticity of human cardiomyocytes in relaxing solutions containing different redox-active molecules (Figure 7).

We subjected single cardiomyocytes to stepwise increases in extension to different sarcomere lengths (SLs) and measured the resulting passive force (Figure 7A; elasticity test). We covered the physiological range of SLs, from 1.8 to 2.4 μ m (Rodriguez et al., 1992). Control experiments showed the expected force profile for a stretched muscle cell, in which a sharp increase in passive force is observed after each step in length, followed by a slow relaxation phase (Figure 7A). It has been proposed that the relaxation of the passive force is caused in part by mechan-

ical unfolding of titin Ig domains (Minajeva et al., 2001; Tskhovrebova et al., 1997; Figure 7A, insets). Consistent with this notion, the amplitude of the relaxation increases at longer SLs, indicating more extensive unfolding at increasing pulling forces.

To induce S-glutathionylation of cryptic cysteines in titin, we incubated the cardiomyocytes for 30 min with 10 mM GSSG at long SLs (2.6–2.7 μ m) that favor Ig domain unfolding (Figure 7A; overstretch). Incubation with GSSG causes substantial softening of the cells, as observed by the marked reduction in the passive force measured during the subsequent elasticity test, which is only \sim 15% of the control force at SLs between 2.2 and 2.4 μ m (Figures 7A and 7B). The force relaxation after a step in length was also severely diminished (Figure 7A, insets). After treatment with GSSG, we changed the buffer to contain 10 mM GSH (SL = 2.6–2.7 μ m) to revert any S-glutathionylation. Treatment with GSH restores the passive force to \sim 75% of the control at 2.2–2.4 μ m SL (Figures 7A and 7B). Normal relaxation kinetics were also recovered (Figure 7A, insets). Because GSH buffers are sensitive to air oxidation and some S-glutathionylated residues can resist treatment with GSH (Gilbert, 1995), we subjected the cells to a final incubation with the strong reducing agent DTT. Incubation with 1 mM DTT makes the cardiomyocytes somewhat stiffer than control cells (Figures 7A and 7B), a result that is compatible with an endogenous basal level of S-glutathionylated cysteines in cardiac titin (Avner et al., 2012).

To distinguish the contribution of cryptic cysteines from that of cysteines that are normally exposed to the solvent, we incubated the cardiomyocytes with 10 mM GSSG, but this time cells were held at slack SL (1.8 μ m) to minimize the extent of titin unfolding. Under these conditions, GSSG only induces a limited decrease in passive force during the elasticity test (Figures 7B and S6A). During incubation at slack SL, the Ig domains of titin remain folded and cryptic cysteines are unreactive toward GSSG. Hence, our results show that the large decrease in cardiomyocyte stiffness is mostly due to S-glutathionylation of cryptic rather than exposed cysteines. The minor changes in elasticity following incubation of slack cardiomyocytes with GSSG are observed mainly at long SLs. We speculate that such variations probably arise from Ig unfolding occurring during the elasticity test itself, which would lead to S-glutathionylation of a small number of cryptic cysteines.

DISCUSSION

Passive tension in cardiac muscle, which is key to the diastolic relaxation of the left ventricle, results to a large degree from the elasticity of the giant sarcomeric protein titin (Linke et al., 1994). Redox signals are widespread in the cardiovascular system and have been shown to modify the elasticity of cardiac tissue, although the underlying molecular mechanisms are unclear. We show here that S-glutathionylation of cryptic cysteines greatly increases the compliance of the I91 domain from cardiac titin via inhibition of folding and weakening of refolded domains. We also demonstrate that results with I91 are generally applicable to many Ig domains in the I-band of titin, because we measure a substantial drop in the passive stiffness of human cardiomyocytes upon S-glutathionylation of cryptic cysteines (Figures 7A, 7B, and S6A). Hence, our findings add to the

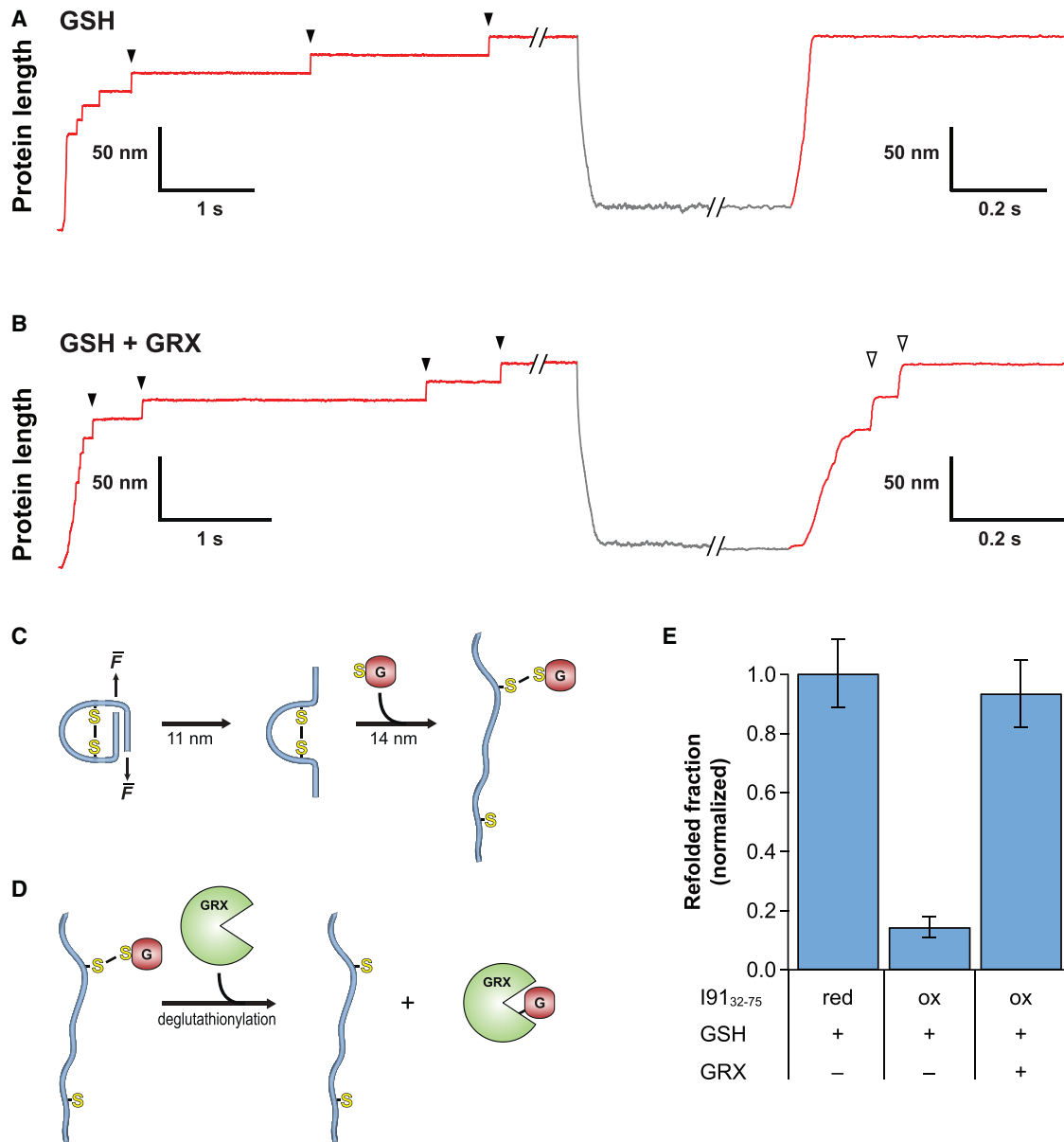


Figure 6. Glutaredoxin Reverses the Mechanical Effects of S-Glutathionylation

(A) I91₃₂₋₇₅ is S-glutathionylated through cleavage of its disulfide by GSH. Unfolding of I91₃₂₋₇₅ increases the protein length by 11 nm, whereas S-glutathionylation increases it further by 14 nm. Exposure-quench-probe pulse protocol probes the refolding of an I91₃₂₋₇₅ polyprotein in the presence of 100 mM GSH. During the exposure pulse, three unfolding events are followed by three S-glutathionylation events (solid arrowheads). The force is then quenched to zero for 5 s. No refolding events are observed during the probe pulse.

(B) Recording showing the unfolding and S-glutathionylation of four I91₃₂₋₇₅ domains in the presence of 100 mM GSH and 45 μM GRX. After a 5 s quench, refolding is apparent during the probe pulse (25 nm steps; open arrowheads).

(C) Diagram of unfolding and S-glutathionylation of I91₃₂₋₇₅. Numbers indicate the associated step sizes detected in force-clamp.

(D) GRX-mediated deglutathionylation.

(E) Refolded fraction after a 5 s quench in 100 mM GSH with or without 45 μM GRX. A baseline for refolding was measured using prereduced I91₃₂₋₇₅ polyprotein in the presence of 100 mM GSH ($n > 90$). Error bars represent SEM.

See also Figure S5.

growing pool of evidence supporting that Ig unfolding controls the elasticity of titin at physiological SLs.

Cryptic cysteines remain inert as long as the parent domains remain folded. Mechanical force accelerates protein unfolding

(Schlierf et al., 2004), which makes cryptic cysteines available for modification. In our experiments, we used high forces in order to trigger rapid unfolding and S-glutathionylation, so that we could observe mechanical effects in a timescale

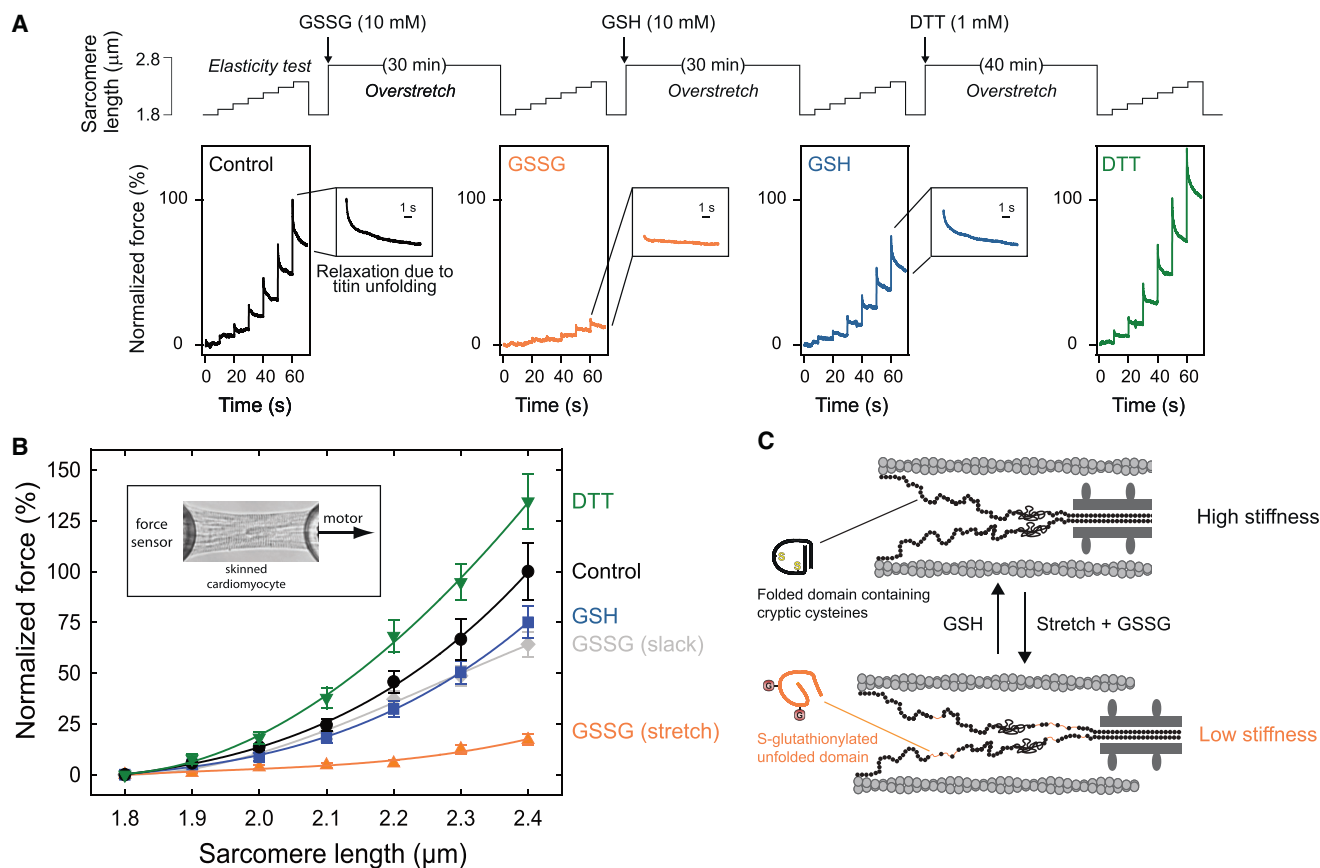


Figure 7. Modulation of Cardiomyocyte Elasticity by S-Glutathionylation of Cryptic Cysteines in Titin

(A) Single human cardiomyocytes were pulled to different sarcomere lengths, and the resulting passive force was measured (elasticity test). Elasticity was probed initially and after subsequent incubations with 10 mM GSSG, 10 mM GSH, and 1 mM DTT; all incubations were done at long sarcomere lengths (2.6–2.7 μm ; overstretch) to induce unfolding of titin Ig domains. Incubation times are indicated. Top trace shows the stretch protocol; bottom trace shows the resulting average passive tension generated by cardiomyocytes. Results are the average of at least eight cells. Insets show magnification of the relaxation phase after stretching the cardiomyocytes to SL = 2.4 μm .

(B) Mean peak force measured at various SLs. GSSG slack is an experiment where incubation with GSSG was done in relaxed cardiomyocytes (SL = 1.8 μm). Forces are normalized to the force measured at 2.4 μm SL in control conditions. Error bars represent SD. Inset: scheme of the experimental setup.

(C) Model of regulation of muscle elasticity through S-glutathionylation of cryptic cysteines in titin.

See also Figure S6.

compatible with single-molecule instrumentation. Whereas the forces we used are higher than forces experienced under normal physiological conditions, even low forces lead to predictable, nonzero rates of mechanical unfolding. To illustrate the interplay between mechanical force and time in the context of modification of cryptic cysteines of titin, we conducted Monte Carlo simulations (Figures S6B–S6H). We simulated the response of a simplified model of titin to a continuous cyclical force protocol between 0.1 and 30 pN, which roughly mimics a human heartbeat (Figure S6B). Individual stretch-relax cycles gave rise to force-extension curves (Figure S6C). As expected from the low forces experienced by titin in the simulations, protein unfolding was only rarely observed. Consequently, the stiffness of titin showed minor variations between subsequent cycles but did not consistently change over a time-scale of hours (Figures S6C and S6F, black trace). After 6 hr of continuous cycles, we introduced 100 mM GSSG. No notice-

able change was observed in the first few cycles after this addition. However, over a time course of hours, the proportion of S-glutathionylated domains increased significantly, leading to persistent unfolded states and decreased titin stiffness (Figures S6D and S6F, red trace). Titin stiffness could be restored to its original value by introduction of GSH (Figure S6E). Simulations further show that the steady-state stiffness of titin depends on the redox potential of the GSH/GSSG buffer (Figure S6G).

Our Monte Carlo simulations suggest that changes in elasticity due to S-glutathionylation of titin probably develop on a time-scale of minutes to hours (Figure S6F). However, other cellular pathways leading to S-glutathionylation are more effective than simple thiol/disulfide exchange and therefore would lead to faster regulation of titin elasticity (Gallogly and Mieyal, 2007). Also, many domains in titin are less mechanically stable than I91 and may thus be more sensitive to S-glutathionylation

(Li et al., 2002). We speculate that, in pathological events where the redox homeostasis changes abruptly, for instance during ischemic episodes (Giordano, 2005), excessive oxidative modification of cryptic cysteines can lead to an aberrant increase in elasticity. However, because modifications of cryptic cysteines do not occur instantly, there may be a window of opportunity for therapeutic intervention to limit damage to the elasticity of heart muscle. In this context, it has been shown that increased titin stiffness leads to diastolic dysfunction (Chung et al., 2013). Our results raise the possibility that cryptic cysteines can be pharmacologically targeted in failing hearts to revert the stiffness of titin back to a physiological range.

We propose that redox-mediated modulation of titin elasticity provides adaptation to the changing chemical status of myocytes in both skeletal and cardiac muscle (Figure 7C). Being able to adjust its own elastic output to the biochemical environment in a use-dependent manner is a fascinating property of titin and constitutes a form of mechanical memory. We are just beginning to understand how such mechanochemical feedback is accomplished. The fact that stretching heart cells activates signaling through reactive oxygen species adds an additional layer of complexity to the interplay between mechanical forces and the redox environment (Prosser et al., 2011). In the case of titin, it will be interesting to examine the mechanical effects of alternative redox posttranslational modifications that compete with S-glutathionylation, such as nitrosylation, sulfenylation, etc.

The mechanomodulatory effects reported here are not necessarily restricted to titin. Cryptic cysteines that become exposed under mechanical loads have recently been identified in elastic proteins of the cytoskeleton and the extracellular matrix, such as spectrin (Johnson et al., 2007; Krieger et al., 2011), ankyrin (Krieger et al., 2011), vimentin (Johnson et al., 2007), fibronectin (Klotzsch et al., 2009), and nuclear lamin-A (Swift et al., 2013). Although commonplace in elastomeric proteins, no regulatory role for cryptic cysteines has been suggested so far. We propose that the modulation of mechanical properties by posttranslational modifications of cryptic residues represents a general mechanism to regulate protein elasticity.

EXPERIMENTAL PROCEDURES

Protein Expression and Purification

The cDNAs coding for 8 mers of I91, the Cys-to-Ala I91 mutants, and I91₃₂₋₇₅ were cloned in the plasmid pQE80 (QIAGEN), and the corresponding polyproteins were purified as described before (Alegre-Cebollada et al., 2011).

Measurement of I91 Cysteine Accessibility to GSSG

A fusion protein SUMO-I91 (0.6 mg/ml) was incubated with 5 mM GSSG at different temperatures for 1 hr. Then, Laemmli sample buffer including 2 mM maleimide was added. Samples were incubated at 90°C for 15 min before SDS-PAGE. The inclusion of 2 mM maleimide ensures that all cysteines that are exposed during denaturation of the sample for SDS-PAGE are blocked and do not react with GSSG. S-alkylation by maleimide is much faster than S-glutathionylation. Control experiments showed that no S-glutathionylation is detected when SUMO-I91 is boiled in the presence of 5 mM GSSG and 2 mM maleimide. To show reversibility by DTT, we incubated the samples with 50 mM DTT at 90°C for 15 min before loading in the SDS-gel. After electrophoresis and western blotting, S-glutathionylation was detected using anti-GSH monoclonal antibodies (Virogen).

Single-Molecule Atomic Force Microscopy

We used custom-built force-clamp AFM setups that have been described in previous publications (Fernandez and Li, 2004) or a commercial force-clamp AFM (Luigs and Neumann; Popa et al., 2013). All AFM experiments were conducted in degassed solution consisting of 10 mM HEPES (pH 7.2), 150 mM NaCl, and 1 mM EDTA. We coated freshly evaporated gold coverslips with the polyprotein of interest by adding a small aliquot (less than 10 μ l) of polyprotein solution (0.2–1 mg/ml). Polyproteins were adsorbed for several minutes on the gold surface. Then, buffer was added to the AFM fluid cell and the experiment was started after in situ calibration of the cantilever using the equipartition theorem (Popa et al., 2013). Single molecules were picked up by pushing the cantilever against the gold surface at a contact force of 0.5–2 nN for 1 s. Then, the piezoelectric actuator was retracted by applying a pulling force. If a tether had been formed, the force rapidly stabilized at the set point. The tether was maintained until the force protocol ended or spontaneous detachment occurred. Refolded fractions were calculated as the ratio between the number of unfolding events in the probe pulse and in the exposure pulse. Once set up, AFM experiments run automatically in the same buffer for hours or even days. We did not observe any changes in the results with time since the start of the experiment, in agreement with I91 cysteines being buried in the fold of the protein (see also Figure 1D).

Data Analysis

Data were analyzed using custom-written software in Igor Pro (Wavemetrics). We included in the analysis traces that showed a fingerprint of two or more unfolding events in the exposure pulse. Only traces that reached the same length at the end of exposure and probe pulses were selected. This criterion ensured that the same molecule was attached in both pulses. Traces showing steps that could not be identified either as unfolding or reduction events were excluded from the analysis. For the I91-Cys63 refolding data, weak and strong refolded domains were quantified from double Gaussian fits to the histograms shown in Figure 4B. In these fits, the widths and centroids were held constant across the data sets, leaving only two free parameters (i.e., the amplitudes of the Gaussians). The numbers of weak and strong domains in each condition were then determined given the total number of folded domains and the relative amplitude of the two Gaussians. In refolding experiments, the number of independent observations N for a particular condition was counted as the total number of protein domains (as observed in the exposure pulse). SEM was estimated using the bootstrap method (Efron, 1982). In the force histograms, N is the number of observations. S-glutathionylation rates were determined from refolding experiments in 100 mM GSSG using the single-cysteine mutants (Figure 4). $k_{47} = 0.33 \text{ M}^{-1}\text{s}^{-1}$ was measured from an exponential fit to the time course of folding inhibition upon exposure to GSSG (gray line in Figure 4C). $k_{63} = 1.6 \text{ M}^{-1}\text{s}^{-1}$ was measured as the average of the rate of disappearance of the strong domains (red line in Figure 4C) and the rate of appearance of the weak domains (blue line in Figure 4C). To examine the GSSG concentration dependency of the reaction, k_{63} was also measured in 10 mM GSSG (Figure 5C). To obtain the refolding fraction of the doubly glutathionylated I91, we fit the data in Figure 3B to the kinetic model in Figure 5A (see Extended Experimental Procedures).

Cardiomyocyte Elasticity Tests

Skinned cardiomyocytes were prepared from deep-frozen human donor heart tissue (Hamdani et al., 2013). Samples were defroze in relaxing solution (in mmol/l: free Mg, 1; KCl, 100; EGTA, 2; Mg-ATP, 4; imidazole, 10 [pH 7.0]), mechanically disrupted and incubated for 5 min in relaxing solution supplemented with 0.5% Triton X-100. The cell suspension was washed five times in relaxing solution. Single cardiomyocytes were selected under an inverted microscope (Zeiss Axiovert 135; 40 \times objective; numerical aperture 0.75) and attached with silicone adhesive to micromanipulator-positioned glass microneedles connected to a force transducer and a piezoelectric motor as part of a "permeabilized myocyte test system" (1600A; with force transducer 403A; Aurora Scientific). SL was monitored using a video camera and analysis software provided by the manufacturer. To measure elasticity, single cardiomyocytes were exposed to stepwise increases in extension from SL = 1.8 μ m (slack) to 2.4 μ m, in increments of 0.1 μ m every 10 s. We included in the final analysis only those cells that were capable of active contractile force generation within 30%

variation compared to the maximum Ca^{2+} -activated force at the start of the experiment. According to this criterion, ~10% of measured cells were discarded. Hence, treatments with GSSG, GSH, and DTT did not induce irreversible damage to the cells.

Experiments with Human or Animal Subjects

The investigation with human samples conformed to the principles outlined in the Declaration of Helsinki and was approved by the Ethics Committee at Ruhr University Bochum (entry 3447-09). Experiments with mouse samples were carried out under the review and approval of the University of Illinois at Chicago Animal Care Committee ACC: 11-229.

SUPPLEMENTAL INFORMATION

Supplemental Information includes Extended Experimental Procedures and six figures and can be found with this article online at <http://dx.doi.org/10.1016/j.cell.2014.01.056>.

AUTHOR CONTRIBUTIONS

J.A.-C., P.K., and J.M.F. conceived the project. J.A.-C., P.K., D.G., E.E., and J.A.R.-P. did the single-molecule experiments. D.G. developed the homology models. J.A.-C. and J.A.R.-P. examined the solvent accessibility of the cysteines of I91. P.K. implemented the Monte Carlo simulations. N.H. and W.A.L. did the cardiomyocyte-stretching experiments. C.M.W. and R.J.S. examined S-glutathionylation of murine titin. J.A.-C., P.K., and J.M.F. wrote the paper.

ACKNOWLEDGMENTS

We thank Sergi Garcia-Manyes for his original observation that mixed disulfides prevent refolding of Ig domains. We thank Thomas Kahn for the SUMO-191 fusion protein. GRX from *E. coli* was a kind gift from Arne Holmgren. Monoclonal antibodies MF20 (D.A. Fischman) and 9D10 (M.L. Greaser) were obtained from the Developmental Studies Hybridoma Bank. This work was supported by the NIH grants HL66030, HL61228 (to J.M.F.), and P01 HL062426 (to R.J.S. and C.M.W.) and grants FP7-MEDIA from the European Union and SFB 1002/TP-B03 from the German Research Foundation (to W.A.L.). J.A.-C. was the recipient of a fellowship from Fundación Ibercaja and a K99 career development award (AI106072) from NIH.

Received: March 8, 2013

Revised: October 17, 2013

Accepted: January 24, 2014

Published: March 13, 2014

REFERENCES

Alegre-Cebollada, J., Kosuri, P., Rivas-Pardo, J.A., and Fernández, J.M. (2011). Direct observation of disulfide isomerization in a single protein. *Nat. Chem.* 3, 882–887.

Anderson, B.R., Bogomolovas, J., Labeit, S., and Granzier, H. (2013). Single molecule force spectroscopy on titin implicates immunoglobulin domain stability as a cardiac disease mechanism. *J. Biol. Chem.* 288, 5303–5315.

Avner, B.S., Shioura, K.M., Scruggs, S.B., Grachoff, M., Geenen, D.L., Helseth, D.L., Jr., Farjah, M., Goldspink, P.H., and Solaro, R.J. (2012). Myocardial infarction in mice alters sarcomeric function via post-translational protein modification. *Mol. Cell. Biochem.* 363, 203–215.

Ceyhan-Birsoy, O., Agrawal, P.B., Hidalgo, C., Schmitz-Abe, K., DeChene, E.T., Swanson, L.C., Soemedi, R., Vasli, N., Iannaccone, S.T., Shieh, P.B., et al. (2013). Recessive truncating titin gene, TTN, mutations presenting as centronuclear myopathy. *Neurology* 81, 1205–1214.

Chen, F.C., and Ogut, O. (2006). Decline of contractility during ischemia-reperfusion injury: actin glutathionylation and its effect on allosteric interaction with tropomyosin. *Am. J. Physiol. Cell Physiol.* 290, C719–C727.

Chung, C.S., Hutchinson, K.R., Methawasini, M., Saripalli, C., Smith, J.E., 3rd, Hidalgo, C.G., Luo, X., Labeit, S., Guo, C., and Granzier, H.L. (2013). Shortening of the elastic tandem immunoglobulin segment of titin leads to diastolic dysfunction. *Circulation* 128, 19–28.

Dalle-Donne, I., Rossi, R., Colombo, G., Giustarini, D., and Milzani, A. (2009). Protein S-glutathionylation: a regulatory device from bacteria to humans. *Trends Biochem. Sci.* 34, 85–96.

del Rio, A., Perez-Jimenez, R., Liu, R., Roca-Cusachs, P., Fernandez, J.M., and Sheetz, M.P. (2009). Stretching single talin rod molecules activates vinculin binding. *Science* 323, 638–641.

Efron, B. (1982). *The Jackknife, the Bootstrap, and Other Resampling Plans* (Philadelphia: SIAM).

Fernandez, J.M., and Li, H. (2004). Force-clamp spectroscopy monitors the folding trajectory of a single protein. *Science* 303, 1674–1678.

Freiburg, A., Trombitas, K., Hell, W., Cazorla, O., Fougerousse, F., Centner, T., Kolmerer, B., Witt, C., Beckmann, J.S., Gregorio, C.C., et al. (2000). Series of exon-skipping events in the elastic spring region of titin as the structural basis for myofibrillar elastic diversity. *Circ. Res.* 86, 1114–1121.

Gallogly, M.M., and Mieval, J.J. (2007). Mechanisms of reversible protein glutathionylation in redox signaling and oxidative stress. *Curr. Opin. Pharmacol.* 7, 381–391.

Gerull, B., Gramlich, M., Atherton, J., McNabb, M., Trombitas, K., Sasse-Klaassen, S., Seidman, J.G., Seidman, C., Granzier, H., Labeit, S., et al. (2002). Mutations of TTN, encoding the giant muscle filament titin, cause familial dilated cardiomyopathy. *Nat. Genet.* 30, 201–204.

Gilbert, H.F. (1990). Molecular and cellular aspects of thiol-disulfide exchange. *Adv. Enzymol. Relat. Areas Mol. Biol.* 63, 69–172.

Gilbert, H.F. (1995). Thiol/disulfide exchange equilibria and disulfide bond stability. *Methods Enzymol.* 251, 8–28.

Giordano, F.J. (2005). Oxygen, oxidative stress, hypoxia, and heart failure. *J. Clin. Invest.* 115, 500–508.

Hamdani, N., Krysiak, J., Kreusser, M.M., Neef, S., Dos Remedios, C.G., Maier, L.S., Krüger, M., Backs, J., and Linke, W.A. (2013). Crucial role for Ca^{2+} /calmodulin-dependent protein kinase-II in regulating diastolic stress of normal and failing hearts via titin phosphorylation. *Circ. Res.* 112, 664–674.

Hare, J.M. (2004). Nitroso-redox balance in the cardiovascular system. *N. Engl. J. Med.* 351, 2112–2114.

Herman, D.S., Lam, L., Taylor, M.R.G., Wang, L.B., Teekakirikul, P., Christodoulou, D., Conner, L., DePalma, S.R., McDonough, B., Sparks, E., et al. (2012). Truncations of titin causing dilated cardiomyopathy. *N. Engl. J. Med.* 366, 619–628.

Itoh-Satoh, M., Hayashi, T., Nishi, H., Koga, Y., Arimura, T., Koyanagi, T., Takahashi, M., Hohda, S., Ueda, K., Nouchi, T., et al. (2002). Titin mutations as the molecular basis for dilated cardiomyopathy. *Biochem. Biophys. Res. Commun.* 291, 385–393.

Johnson, C.P., Tang, H.Y., Carag, C., Speicher, D.W., and Discher, D.E. (2007). Forced unfolding of proteins within cells. *Science* 317, 663–666.

Kellermayer, M.S., and Grama, L. (2002). Stretching and visualizing titin molecules: combining structure, dynamics and mechanics. *J. Muscle Res. Cell Motil.* 23, 499–511.

Klotzsch, E., Smith, M.L., Kubow, K.E., Muntwyler, S., Little, W.C., Beyeler, F., Gourdon, D., Nelson, B.J., and Vogel, V. (2009). Fibronectin forms the most extensible biological fibers displaying switchable force-exposed cryptic binding sites. *Proc. Natl. Acad. Sci. USA* 106, 18267–18272.

Kosuri, P., Alegre-Cebollada, J., Feng, J., Kaplan, A., Ingles-Prieto, A., Badilla, C.L., Stockwell, B.R., Sanchez-Ruiz, J.M., Holmgren, A., and Fernandez, J.M. (2012). Protein folding drives disulfide formation. *Cell* 151, 794–806.

Krieger, C.C., An, X., Tang, H.Y., Mohandas, N., Speicher, D.W., and Discher, D.E. (2011). Cysteine shotgun-mass spectrometry (CS-MS) reveals dynamic sequence of protein structure changes within mutant and stressed cells. *Proc. Natl. Acad. Sci. USA* 108, 8269–8274.

- Li, H., Linke, W.A., Oberhauser, A.F., Carrion-Vazquez, M., Kerkvliet, J.G., Lu, H., Marszalek, P.E., and Fernandez, J.M. (2002). Reverse engineering of the giant muscle protein titin. *Nature* *418*, 998–1002.
- Lillig, C.H., Berndt, C., and Holmgren, A. (2008). Glutaredoxin systems. *Biochim. Biophys. Acta* *1780*, 1304–1317.
- Linke, W.A., and Krüger, M. (2010). The giant protein titin as an integrator of myocyte signaling pathways. *Physiology (Bethesda)* *25*, 186–198.
- Linke, W.A., Popov, V.I., and Pollack, G.H. (1994). Passive and active tension in single cardiac myofibrils. *Biophys. J.* *67*, 782–792.
- Lovelock, J.D., Monasky, M.M., Jeong, E.M., Lardin, H.A., Liu, H., Patel, B.G., Taglieri, D.M., Gu, L., Kumar, P., Pokhrel, N., et al. (2012). Ranolazine improves cardiac diastolic dysfunction through modulation of myofilament calcium sensitivity. *Circ. Res.* *110*, 841–850.
- Martínez-Ruiz, A., and Lamas, S. (2007). Signalling by NO-induced protein S-nitrosylation and S-glutathionylation: convergences and divergences. *Cardiovasc. Res.* *75*, 220–228.
- Matsumoto, Y., Hayashi, T., Inagaki, N., Takahashi, M., Hiroi, S., Nakamura, T., Arimura, T., Nakamura, K., Ashizawa, N., Yasunami, M., et al. (2005). Functional analysis of titin/connectin N2-B mutations found in cardiomyopathy. *J. Muscle Res. Cell Motil.* *26*, 367–374.
- Mayans, O., Wuerges, J., Canela, S., Gautel, M., and Wilmanns, M. (2001). Structural evidence for a possible role of reversible disulphide bridge formation in the elasticity of the muscle protein titin. *Structure* *9*, 331–340.
- McNally, E.M. (2012). Genetics: broken giant linked to heart failure. *Nature* *483*, 281–282.
- Minajeva, A., Kulke, M., Fernandez, J.M., and Linke, W.A. (2001). Unfolding of titin domains explains the viscoelastic behavior of skeletal myofibrils. *Biophys. J.* *80*, 1442–1451.
- Mollica, J.P., Dutka, T.L., Merry, T.L., Lamboley, C.R., McConell, G.K., McKenna, M.J., Murphy, R.M., and Lamb, G.D. (2012). S-glutathionylation of troponin I (fast) increases contractile apparatus Ca²⁺ sensitivity in fast-twitch muscle fibres of rats and humans. *J. Physiol.* *590*, 1443–1463.
- Nedrud, J., Labeit, S., Gotthardt, M., and Granzier, H. (2011). Mechanics on myocardium deficient in the N2B region of titin: the cardiac-unique spring element improves efficiency of the cardiac cycle. *Biophys. J.* *101*, 1385–1392.
- Norton, N., Li, D., Rampersaud, E., Morales, A., Martin, E.R., Zuchner, S., Guo, S., Gonzalez, M., Hedges, D.J., Robertson, P.D., et al.; National Heart, Lung, and Blood Institute GO Exome Sequencing Project and the Exome Sequencing Project Family Studies Project Team (2013). Exome sequencing and genome-wide linkage analysis in 17 families illustrate the complex contribution of TTN truncating variants to dilated cardiomyopathy. *Circ Cardiovasc Genet* *6*, 144–153.
- Pfeffer, M.A., and Braunwald, E. (1990). Ventricular remodeling after myocardial infarction. Experimental observations and clinical implications. *Circulation* *81*, 1161–1172.
- Popa, I., Kosuri, P., Alegre-Cebollada, J., Garcia-Manyes, S., and Fernandez, J.M. (2013). Force dependency of biochemical reactions measured by single-molecule force-clamp spectroscopy. *Nat. Protoc.* *8*, 1261–1276.
- Prosser, B.L., Ward, C.W., and Lederer, W.J. (2011). X-ROS signaling: rapid mechano-chemo transduction in heart. *Science* *333*, 1440–1445.
- Rastaldo, R., Pagliaro, P., Cappello, S., Penna, C., Mancardi, D., Westerhof, N., and Losano, G. (2007). Nitric oxide and cardiac function. *Life Sci.* *81*, 779–793.
- Rodriguez, E.K., Hunter, W.C., Royce, M.J., Leppo, M.K., Douglas, A.S., and Weisman, H.F. (1992). A method to reconstruct myocardial sarcomere lengths and orientations at transmural sites in beating canine hearts. *Am. J. Physiol.* *263*, H293–H306.
- Sánchez, G., Pedrozo, Z., Domenech, R.J., Hidalgo, C., and Donoso, P. (2005). Tachycardia increases NADPH oxidase activity and RyR2 S-glutathionylation in ventricular muscle. *J. Mol. Cell. Cardiol.* *39*, 982–991.
- Schlierf, M., Li, H., and Fernandez, J.M. (2004). The unfolding kinetics of ubiquitin captured with single-molecule force-clamp techniques. *Proc. Natl. Acad. Sci. USA* *101*, 7299–7304.
- Smith, M.L., Gourdon, D., Little, W.C., Kubow, K.E., Eguiluz, R.A., Luna-Morris, S., and Vogel, V. (2007). Force-induced unfolding of fibronectin in the extracellular matrix of living cells. *PLoS Biol.* *5*, e268.
- Somkuti, J., Mártonfalvi, Z., Kellermayer, M.S., and Smeller, L. (2013). Different pressure-temperature behavior of the structured and unstructured regions of titin. *Biochim. Biophys. Acta* *1834*, 112–118.
- Swift, J., Ivanovska, I.L., Buxboim, A., Harada, T., Dingal, P.C., Pinter, J., Pajeroski, J.D., Spinler, K.R., Shin, J.W., Tewari, M., et al. (2013). Nuclear lamin-A scales with tissue stiffness and enhances matrix-directed differentiation. *Science* *341*, 1240104.
- Taylor, M., Graw, S., Sinagra, G., Barnes, C., Slavov, D., Brun, F., Pinamonti, B., Salcedo, E.E., Sauer, W., Pyxaras, S., et al. (2011). Genetic variation in titin in arrhythmogenic right ventricular cardiomyopathy-overlap syndromes. *Circulation* *124*, 876–885.
- Trombitás, K., Greaser, M., Labeit, S., Jin, J.P., Kellermayer, M., Helmes, M., and Granzier, H. (1998). Titin extensibility in situ: entropic elasticity of permanently folded and permanently unfolded molecular segments. *J. Cell Biol.* *140*, 853–859.
- Tskhovrebova, L., Trinick, J., Sleep, J.A., and Simmons, R.M. (1997). Elasticity and unfolding of single molecules of the giant muscle protein titin. *Nature* *387*, 308–312.
- Warren, C.M., Krzesinski, P.R., and Greaser, M.L. (2003). Vertical agarose gel electrophoresis and electroblotting of high-molecular-weight proteins. *Electrophoresis* *24*, 1695–1702.
- West, M.B., Hill, B.G., Xuan, Y.T., and Bhatnagar, A. (2006). Protein glutathionylation by nitric oxide: an intracellular mechanism regulating redox protein modification. *FASEB J.* *20*, 1715–1717.
- Wiita, A.P., Ainavarapu, S.R., Huang, H.H., and Fernandez, J.M. (2006). Force-dependent chemical kinetics of disulfide bond reduction observed with single-molecule techniques. *Proc. Natl. Acad. Sci. USA* *103*, 7222–7227.
- Wu, C., Belenda, C., Leroux, J.C., and Gauthier, M.A. (2011). Interplay of chemical microenvironment and redox environment on thiol-disulfide exchange kinetics. *Chemistry* *17*, 10064–10070.